

Diurnal dynamics of nonphotochemical quenching in *Arabidopsis npq* mutants assessed by solar-induced fluorescence and reflectance measurements in the field

Kelvin Acebron , Shizue Matsubara , Christoph Jedmowski , Dzhane Emin, Onno Muller  and Uwe Rascher 

Plant Sciences (IBG-2), Forschungszentrum Jülich GmbH, Jülich D-52425, Germany

Authors for correspondence:

Kelvin Acebron

Email: k.acebron@fz-juelich.de

Uwe Rascher

Email: u.rascher@fz-juelich.de

Received: 16 March 2020

Accepted: 18 September 2020

New Phytologist (2021) 229: 2104–2119

doi: 10.1111/nph.16984

Key words: chlorophyll fluorescence, diurnal and seasonal regulation, nonphotochemical quenching (NPQ), photochemical reflectance index (PRI), photoinhibition, photosystem (PSII) efficiency, solar-induced fluorescence (SIF), violaxanthin-antheraxanthin-zeaxanthin (VAZ) cycle.

Summary

- Solar-induced fluorescence (SIF) is highly relevant in mapping photosynthesis from remote-sensing platforms. This requires linking SIF to photosynthesis and understanding the role of nonphotochemical quenching (NPQ) mechanisms under field conditions. Hence, active and passive fluorescence were measured in *Arabidopsis* with altered NPQ in outdoor conditions.
- Plants with mutations in either violaxanthin de-epoxidase (*npq1*) or PsbS protein (*npq4*) exhibited reduced NPQ capacity. Parallel measurements of NPQ, photosystem II efficiency, SIF and spectral reflectance (ρ) were conducted diurnally on one sunny summer day and two consecutive days during a simulated cold spell.
- Results showed that both *npq* mutants exhibited higher levels of SIF compared to wild-type plants. Changes in reflectance were related to changes in the violaxanthin–antheraxanthin–zeaxanthin cycle and not to PsbS-mediated conformational changes. When plants were exposed to cold temperatures, rapid onset of photoinhibition strongly quenched SIF in all lines.
- Using well-characterized *Arabidopsis npq* mutants, we showed for the first time the quantitative link between SIF, photosynthetic efficiency, NPQ components and leaf reflectance. We discuss the functional potential and limitations of SIF and reflectance measurements for estimating photosynthetic efficiency and NPQ in the field.

Introduction

The global mapping of ecosystem functions largely relies on an understanding of the functional meaning of solar-induced fluorescence (SIF) and plant spectral reflectance (ρ). Solar-induced fluorescence signal has been successfully measured at leaf level (van Wittenberghe *et al.*, 2013; Magney *et al.*, 2017; Vilfan *et al.*, 2019), at the top of the canopy (Pinto *et al.*, 2016), in airborne systems (Zarco-Tejada *et al.*, 2000; Rascher *et al.*, 2015) and from satellite platforms (Frankenberg *et al.*, 2011; Joiner *et al.*, 2011). There are therefore increasing opportunities for understanding plant photosynthesis in natural environments on different scales (Rascher *et al.*, 2009). Several studies have demonstrated the sensitivity of SIF to major abiotic stress conditions (Ač *et al.*, 2015), absorbed photosynthetically active radiation (APAR; Yang *et al.*, 2015) and photosynthetic efficiency (Rossini *et al.*, 2015; Pinto *et al.*, 2016). As a passive signal, the potential mapping of SIF on a large scale is clearly a novel advantage for global studies. Several existing satellites, such as GOSAT (Frankenberg *et al.*, 2011), MERIS (García-Plazaola *et al.*, 2007), GOME-2 (Joiner *et al.*, 2011), Sentinel-5 Precursor, TROPOMI (Kohler *et al.*, 2018), Tansat (Du *et al.*, 2018) and OCO-2

(Frankenberg *et al.*, 2011; Sun *et al.*, 2018) are capable of providing SIF at global scales by spatially and temporally aggregating existing satellite data. Because of the potential of SIF to deliver information about actual photosynthesis, Fluorescence Explorer (FLEX) was selected as the 8th Explorer satellite mission of the European Space Agency, to provide timely maps of SIF and ρ to understand terrestrial photosynthesis on a global scale (Drusch *et al.*, 2016).

Because the fundamental relationships between Chl fluorescence, photochemistry and heat dissipation are dynamic, linking SIF to photosynthesis (or photochemistry in the context of this study) requires a holistic understanding of the interplay between nonphotochemical quenching (NPQ) mechanisms operating in field conditions. Nonphotochemical quenching involves thermal dissipation of excess absorbed energy. When leaves experience an increase in light intensity, thylakoid lumen becomes acidic, which protonates PsbS protein and activates violaxanthin de-epoxidase (VDE) to convert violaxanthin (V) to zeaxanthin (Z) via antheraxanthin (A) in the VAZ cycle. Violaxanthin de-epoxidase is also capable of converting lutein epoxide (Lx) to lutein (L) in species in which the lutein epoxide–lutein cycle operates (García-Plazaola *et al.*, 2007). Under these conditions, conformational change

in the major light-harvesting antenna complex (LHCII) of photosystem II (PSII) are induced, switching the functional mode from light harvesting to heat dissipation (for a review, see Goss & Lepetit, 2015; Ruban, 2016). Different components of NPQ are defined by their relaxation kinetics upon darkening, namely energy-dependent quenching (qE), zeaxanthin-dependent quenching (qZ) and photoinhibitory quenching (qI). Rapidly inducible and reversible qE is the predominant form of NPQ in higher plants. Energy-dependent quenching is activated and deactivated within seconds to minutes and thus responds to light fluctuations (Müller *et al.*, 2001). *Arabidopsis* mutants without qE were found to lack PsbS protein (*npq4*) and apparently also conformational change in LHCII (Li *et al.*, 2000). In addition, NPQ is dependent on Z (Demmig-Adams, 1990). The part of NPQ which is solely dependent on Z and does not require acidic lumen was eventually termed qZ (Jahns & Holzwarth, 2012). It has been speculated that Z is either capable of directly quenching the singlet excited state of Chl*a* (Owens *et al.*, 1992) or altering the conformation of LHCII (Horton *et al.*, 1991). The qZ component relaxes more slowly than qE, taking several minutes to an hour in the dark. *Arabidopsis npq1* mutants lacking VDE (Niyogi *et al.*, 1998) are deficient in light-induced Z formation and thus have less photoprotective capacity (Havaux & Niyogi, 1999). The third type, qI, is a slowly reversible component of NPQ, also known as sustained NPQ, and is associated with Z retention (Demmig-Adams & Adams, 2006) and takes several hours to relax. Photoinhibitory quenching is characterized by reduced maximal photochemical efficiency (F_v/F_m ; Krause, 1988) and increased energy dissipation within PSII (Krause & Weis, 1991). Reduction and recovery of F_v/F_m were shown to be associated with inactivation and repair of PSII, respectively (Greer *et al.*, 1991).

The mechanistic interplay between fluorescence yield (F_{yield}), NPQ and the effective quantum yield of PSII (Φ_{PSII}) can be quantified using a pulse-amplitude modulation (PAM) fluorometer (Krause & Weis, 1991; Maxwell & Johnson, 2000). At leaf level, there is a clear negative relationship between NPQ and Φ_{PSII} over the course of a day, protecting plants from excess light (i.e. photoprotection). Studies carried out in nonstressful conditions have shown that Φ_{PSII} decreases while NPQ increases with increasing light intensity. This relationship is tightly linked to the de-epoxidation state of the VAZ cycle (Demmig-Adams *et al.*, 1995). In winter, sustained NPQ predominates, especially in overwintering evergreen plants (Öquist & Huner, 2003; Verhoeven, 2014).

NPQ is quantified from the maximal fluorescence in dark-adapted (F_m) and light-adapted (F_m') states measured during short strong light pulses which saturate photochemical quenching (qP, see Eqn 3; Bilger & Björkman, 1990). While Magney *et al.* (2019) have shown that spectral changes in SIF at leaf level were attributed to a rather small contribution of NPQ, the effects of different NPQ components (qE, qZ and qI) have not been resolved. In remote sensing, the photochemical reflectance index (PRI) is used to track changes in the composition of the VAZ-cycle pigments (Gamon *et al.*, 1990). In drought-stressed tobacco, Alonso *et al.* (2017) showed how diurnal dynamics of NPQ are related to changes in PRI and SIF. Zeaxanthin formation

increases absorbance at 505 nm, and changes in LHCII conformation alter the absorbance at 535 nm (Krause, 1973; Bilger & Björkman, 1994). This creates opportunities to measure ρ in leaves and thereby monitor the interconversion between V and Z (Gamon & Surfus, 1999). Correlation between PRI and NPQ was validated *in situ* using *Arabidopsis npq1* and *npq4* mutants. Using these mutants, Kohzuma & Hikosaka (2018) found that PRI is capable of tracking qZ but not the total NPQ activity. Notably, they proposed that PRI is sensitive to changes in luminal pH. However, the limitation of PRI in tracking interconversion between V and Z, which is relevant for the changes in NPQ, lies in its sensitivity to long-term or seasonal changes in carotenoid : Chl ratio (Wong & Gamon, 2014), leaf albedo (Busch *et al.*, 2009; Wong & Gamon, 2014) and canopy structure (Barton & North, 2001; Garbulsky *et al.*, 2011). Nevertheless, Nichol *et al.* (2006) proposed that PRI can potentially account for 70% of the total NPQ, assuming that 70% of the total NPQ is dependent on Z accumulation. Furthermore, van Wittenberghe *et al.* (2019) suggested that changes in light absorbance (a fast response for 500–570 nm and an occasional slow response at *c.* 550 nm and *c.* 750 nm) upon illumination at leaf level may be attributable to structural adjustments of photosynthetic membranes involving both carotenoids and Chls. If PRI and ρ can detect changes in the luminal pH and LHCII conformation at leaf level, it may be possible to monitor the qE component of NPQ remotely.

Because SIF reflects both photochemical and nonphotochemical quenching events, it does not linearly correlate with photosynthesis. Using the Soil-Canopy Observation, Photosynthesis and Energy Balance (SCOPE) model, van der Tol *et al.* (2014) demonstrated the effect of relative light saturation on the relationship between F_{yield} and photochemical yield (Φ_p). In low light, the relationship between F_{yield} and Φ_p is negative. Maguire *et al.* (2020) recently confirmed that this negative relationship between F_{yield} and Φ_p under low light was determined by photosynthetic induction at the canopy scale under field conditions. In high light, on the other hand, F_{yield} and Φ_p can decrease concomitantly due to the activation of NPQ. Under severe stress, however, they showed that F_{yield} may increase as Φ_p decreases. Despite these complex relationships between F_{yield} and Φ_p , the power of the SCOPE model has been demonstrated by predicting the net canopy photosynthesis using SIF retrieved at O₂A and O₂B bands (Verrelst *et al.*, 2016).

Atherton *et al.* (2016) showed that combining SIF with PRI can predict the dynamics of photochemical and nonphotochemical activities at leaf level. Although the integration of leaf-level gas-exchange parameters has led to great progress and improvements in modelling, its application is still limited to healthy and not chronically photoinhibited leaves (Hikosaka & Noda, 2018). Recent efforts to link active and passive fluorescence signals with CO₂ uptake have led to the development of tools which help us advance our understanding of the relationship between SIF and the photosynthetic processes in leaves (Magney *et al.*, 2017; Vilfan *et al.*, 2019). Also, Pinto *et al.* (2016) recently provided a proof of concept demonstrating that SIF images captured at the top of the canopy can visualize spatial and temporal variation in

photosynthetic efficiency (Φ_{PSII}). Since canopy photosynthesis occurs via a totality of individual leaf parts, an understanding of spatio-temporal variation of photosynthesis at leaf level is of fundamental importance. In the context of the FLEX satellite mission (Drusch *et al.*, 2016), it is necessary to understand the influence of NPQ on SIF and ρ in order to correctly estimate photosynthesis or gross primary productivity (GPP). However, quantitative data describing the link between photosynthesis (Φ_{PSII}), SIF, NPQ and ρ are still scarce and inconclusive, mainly due to the composite nature of fluorescence quenching (i.e. different NPQ components and qP).

The objective of this study is to provide a mechanistic understanding of the link between photochemical/nonphotochemical fluorescence quenching and remote-sensing signals. We used well-established *Arabidopsis* *npq* mutants (*npq4* and *npq1*) to evaluate the effects of qE, qZ, qI and the formation of Z on SIF and ρ . The experiments were conducted on a sunny summer day (qE and qZ dominate NPQ) and two consecutive days during a simulated cold spell (also, qI influences NPQ). Specifically, the following questions were asked: How do different NPQ components (qE, qZ and qI) affect the emission of SIF as well as leaf ρ ? How much do Φ_{PSII} and NPQ contribute to diurnal SIF variations under conditions of high light and sudden transfer to cold temperatures (i.e. a simulated cold spell)? And what NPQ components can be quantitatively estimated by diurnal measurements of leaf ρ and SIF emission? Our results show, for the first time, the link between active and passive fluorescence signals along with plant ρ during NPQ variations under high light and cold stress in outdoor conditions.

Materials and Methods

Arabidopsis mutants and growth conditions

Arabidopsis thaliana Col-0 ecotype seeds, VDE-deficient (*npq1*; Niyogi *et al.*, 1998) and PsbS-deficient (*npq4*; Li *et al.*, 2000) mutant seeds (derived from mutagenesis using either ethyl methanesulfonate or fast-neutron bombardment) were sown and transplanted into small pots (0.34 l) containing *Dachstaudensubstrat* soil (Hawita, Vechta, Germany). The seedlings were grown in a growth chamber with a 12 h : 12 h, light : dark photoperiod ($100 \mu\text{mol}_{\text{photon}} \text{m}^{-2} \text{s}^{-1}$), with the temperature set to 20°C during the day and 15°C during the night. Relative humidity was maintained at 60% (Supporting Information Fig. S1). Plants were transferred to the glasshouse *c.* 20 d after sowing. In summer, plants were placed outside for at least two consecutive days before measurements were taken. In winter, plants were directly exposed to the elements outside, and diurnal measurements were conducted on two consecutive days (keeping the plants in the glasshouse at night).

Active fluorescence measurement using PAM and LIFT

Fluorescence yield, Φ_{PSII} and NPQ were measured in five plants of each plant type using the Imaging-PAM M-Series (Walz, Effeltrich, Germany) and LIFT instrument (LIFT-REM version,

Soliense Inc., New York, NY, USA). During light induction, actinic light was set to *c.* $370 \mu\text{mol}_{\text{photon}} \text{m}^{-2} \text{s}^{-1}$, while in PAM, the measuring light and saturating pulse were at $< 1 \mu\text{mol}_{\text{photon}} \text{m}^{-2} \text{s}^{-1}$ and $> 5000 \mu\text{mol}_{\text{photon}} \text{m}^{-2} \text{s}^{-1}$ for 800 ms, respectively.

All plants were dark-adapted for at least 1 h when minimal fluorescence (F_0) and F_m were measured. A light-induction curve was determined by illuminating the plant continuously for 5 min while F_m was recorded every 20 s. All fluorescence images were analysed using IMAGINGWIN Software (Walz, Germany), and the mean value was derived as the average of all selected pixels of the plant image. (see Table S1 for a list of abbreviations).

The LIFT instrument was equipped with a pulse-controlled blue LED (445 nm) excitation source, which was focused on a 2-cm measuring spot. Fluorescence was detected at $685 (\pm 10)$ nm in the coaxial optical path of the instrument. Measurement was based on the fast repetition-rate principle (Kolber *et al.*, 1998) (capable of saturating the primary electron acceptor of PSII (Q_A)) and is called the Q_A flash protocol (Osmond *et al.*, 2017). Our measurement protocol was 209.75 ms, which produced 300 flashlets from 0.75 ms of the induction phase and 127 flashlets from 209 ms of the relaxation phase. Fluorescence emission was calculated by subtracting the signal for the inter-flashlet periods from the in-flashlet fluorescence signal. Finally, F_{yield} (F_{LIFT}) was derived by normalizing the fluorescence emission against the constant excitation power.

The LIFT sensor was situated at a distance of 60 cm, approximately in the nadir position relative to the plant target. In the laboratory, LIFT parameters were traced every 5 s for a duration of 5 min using the Q_A flash protocol while actinic illumination was turned on. Values for traced parameters were averaged every 40 s. During outdoor measurements, an average of the two simultaneous Q_A flashes was used to quantify Φ_{PSII} and NPQ of light-adapted plants.

Measurement of SIF spectra, F687 and F760

Full-SIF spectra were measured in three detached leaves of each plant type using a FieldSpec 4 Wide-Res Spectroradiometer (Analytical Spectral Devices (ASD), Boulder, CO, USA) coupled to a FluoWat leaf clip (van Wittenbergh *et al.*, 2013), integrated with a short-pass band filter (> 650 nm). The ASD FieldSpec device has a wavelength range of 350–2500 nm, with a resolution of 3 nm at 700 nm and 30 nm at 1400/2100 nm. A scanning time of 100 ms was used, and 10 readings were averaged per log. The measurement protocol for detecting SIF spectra was based on that described in a study by van Wittenbergh *et al.* (2013). In contrast, SIF at 687 nm (F687) and 760 nm (F760) were measured using a FLOX device (JB Hyperspectral Devices, Düsseldorf, Germany) and retrieved using an improved Fraunhofer line depth (iFLD) method (Alonso *et al.*, 2008).

Measurement of plant reflectance

Diurnal changes in plant ρ were measured with a point spectrometer (Flame; Ocean Optics, FL, USA) integrated

within the FLOX device. The FLOX fibre optics were set orthogonally to the plant at a distance of 5 cm (for the measurement setup, see Fig. S2). The upwelling and downwelling fibre-optic channels had a field of view of 180° and 25°, respectively.

Measuring the diurnal response of Arabidopsis plants in outdoor conditions on a summer day and during a simulated cold spell

To quantify the diurnal changes, magnitudes and relationships among SIF, Φ_{PSII} and NPQ, parallel measurements of active and passive fluorescence parameters were conducted outdoors under a clear sky on a summer day and on two consecutive winter days.

Four plants of each type were measured in the summer (28 August 2017) from 07:34 to 16:04 h with a daytime temperature range from 19.7°C (minimum) to 31.5°C (maximum). In winter, three plants were measured from 09:37 to 16:50 h on day 1 (22 February 2018, −0.8 to 4.1°C) and from 07:00 to 16:30 h on day 2 (23 February 2018, −3.9 to 3.3°C). All plants were randomized for each measurement window to remove the bias associated with temporal changes that may affect both optical and physiological plant responses. Outdoor measurements were performed at the Plant Science Department of the Research Center, Jülich, Germany (lat 50°54'35.4"N, long 6°24'45.5"E). Recorded diurnal light intensity and temperature for both summer and winter conditions are summarized in Fig. S3.

Tracing recovery of PSII efficiency in glasshouse conditions

Recovery of F_v/F_m (Eqn 1) was traced in glasshouse plants exposed to the cold. Three plants of each type were transferred to the glasshouse the day after measurements during a winter spell. Plants were dark-adapted for at least 30 min before F_v/F_m measurement, and measurements were taken every c. 45 mins for a duration of 3.5 h. As in the laboratory and outdoor measurements, the Q_A flash protocol was used for the LIFT device to estimate the F_v/F_m parameter.

Calculation of active fluorescence parameters and remote-sensing signals

Active fluorescence parameters derived from PAM were calculated using Eqns 1–3, based on Maxwell & Johnson (2000). In the case of LIFT measurements, F_{0_LIFT} was equal to the first fluorescence transient recorded upon the first excitation flashlet of the Q_A protocol, while F_{m_LIFT} was the average F_{LIFT} recorded in 301 and 302 flashlets. All LIFT data were collected and analysed based on the method described by Keller *et al.* (2019).

$$F_v/F_m = \frac{(F_m - F_0)}{F_m} \quad \text{Eqn 1}$$

$$\Phi_{\text{PSII}} = \frac{F'_m - F'}{F'_m} \quad \text{Eqn 2}$$

$$NPQ = \frac{F_m - F'_m}{F'_m} \quad \text{Eqn 3}$$

Passive fluorescence was quantified using either the FluoWat device or the FLOX system. Solar-induced fluorescence and $\text{SIF}_{\text{yield}}$ from the FluoWat device were derived as described previously (van Wittenberghe *et al.*, 2013), and F687 and F760 derived from FLOX measurements were normalised to the photosynthetically active radiation (PAR) to estimate solar-induced fluorescence yield at 687 nm ($\text{F687}_{\text{yield}}$) and 760 nm ($\text{F760}_{\text{yield}}$), respectively.

Reflectance from 400 to 750 nm was calculated from the FLOX diurnal measurements by normalizing reflected radiance to the incoming irradiance. Reflectance values were further adjusted based on the minimum and maximum ρ values for each measurement:

$$\rho_{\text{adj}} = \frac{\rho_{\lambda} - \rho_{\min}}{\rho_{\max} - \rho_{\min}} \quad \text{Eqn 4}$$

Using the adjusted ρ , the photochemical reflectance index (PRI) was calculated based on the equation given in a study by Gamon *et al.* (1992).

$$\text{PRI}_{570} = \frac{\rho_{531} - \rho_{570}}{\rho_{531} + \rho_{570}} \quad \text{Eqn 5}$$

Statistical analysis

A completely randomized design was used in the laboratory setup, and a repeated measures design was used in the diurnal outdoor setup. The models were fitted using the *lmer* function in R (R Core Team, 2013), where genotypes and the time of measurements were denoted as fixed effects and replicates as random effects. Pairwise mean comparisons were made using the *lsmeans* function.

For cluster analysis, the adjusted ρ data were pooled, consisting of individual measurements from four plants of each plant type from all measurement points taken throughout the entire day in the summer. Dissimilarity between data points was computed in R using Pearson's R^2 in the *dist* function. Hierarchical clustering was computed using the *hclust* function (Ward's method). The correlation coefficient (r) values for average points between SIF and NPQ, SIF and PRI, and SIF and Φ_{PSII} , were calculated using the *cor.test* function in R using Pearson's method.

Results

Effect of reduced NPQ on active Chl-fluorescence parameters

To characterize the photochemical and nonphotochemical responses of *npq* mutants, active fluorescence parameters were

traced on dark-adapted plants during photosynthetic induction. Fluorescence yield in both *npq* mutants was higher than in the Arabidopsis wild-type (WT) which is more pronounced in the steady-state condition (Fig. 1a). By contrast, Φ_{PSII} was similar in the mutant and WT plants (Fig. 1b), while the degree of NPQ for both mutants was lower (Fig. 1c). Moreover, the level of NPQ in the *npq1* mutants increased abruptly, while *npq4* showed a gradually increasing trend. Absolute values of PAM and LIFT were different (see discussion in Pieruschka *et al.*, 2014 on this methodological difference); however, relative changes showed the same dynamics. Despite the difference in F_{yield} , no morphological differences in size or greenness were observed between the WT and mutants (data not shown).

Diurnal trend of PSII efficiency, NPQ and SIF in summer and winter conditions

To investigate the link between SIF, Φ_{PSII} and NPQ in the field, active and passive fluorescence were simultaneously measured in an outdoor scenario throughout the course of the day. During the day in summer, for all plant types, Φ_{PSII} was negatively correlated with incoming PAR, whereas NPQ was positively correlated with incoming PAR (Fig. 2a, b). The lowest value of Φ_{PSII} was observed at midday, when the light intensity was at its peak, while NPQ was highest at the end of the day. The effective quantum yield of PSII for both mutants was significantly lower than that of the WT (Table S2). Almost invariably throughout the day, NPQ was lower for both mutants than it was for the WT. Like NPQ, SIF followed the diurnal course of PAR; that is, F760 was highest at midday, and lowest in the early morning and late afternoon. While this trend was found to apply to all the plant types, the *npq* mutants had higher SIF emission than the WT (Fig. 2c). Conversely, F760_{yield} in the WT showed high values in the morning and late afternoon, and the lowest values at midday (Fig. 2d). F760_{yield} in mutants was higher than the WT but tended to decrease towards the end of the day (Fig. 2d). At the end of the day, this decrease coincided with significantly lower Φ_{PSII} in the mutants, compared to the WT (Table S2).

During the winter spell, Φ_{PSII} for all plant types immediately decreased as soon as the plants were exposed to sudden cold treatment (Fig. 3a). At the end of the day, F_v/F_m decreased to less than half its initial value (Fig. 3a, marked with an asterisk). While Φ_{PSII} dropped rapidly after exposure to the cold, NPQ gradually increased over the course of the day (Fig. 3b). In addition, *npq* mutants showed different levels of NPQ to those of the WT. Accordingly, differences in F760 were also observed between mutants and the WT, but these were only evident between the initial hours of exposure to the cold and midday (Fig. 3c). Thereafter, F760 was quenched in line with the other plant types. Interestingly, F760 emission followed a similar diurnal trend to F760_{yield}, with both being independent of the diurnal PAR (Fig. 3c,d). Notably, the quenched state was sustained until the second

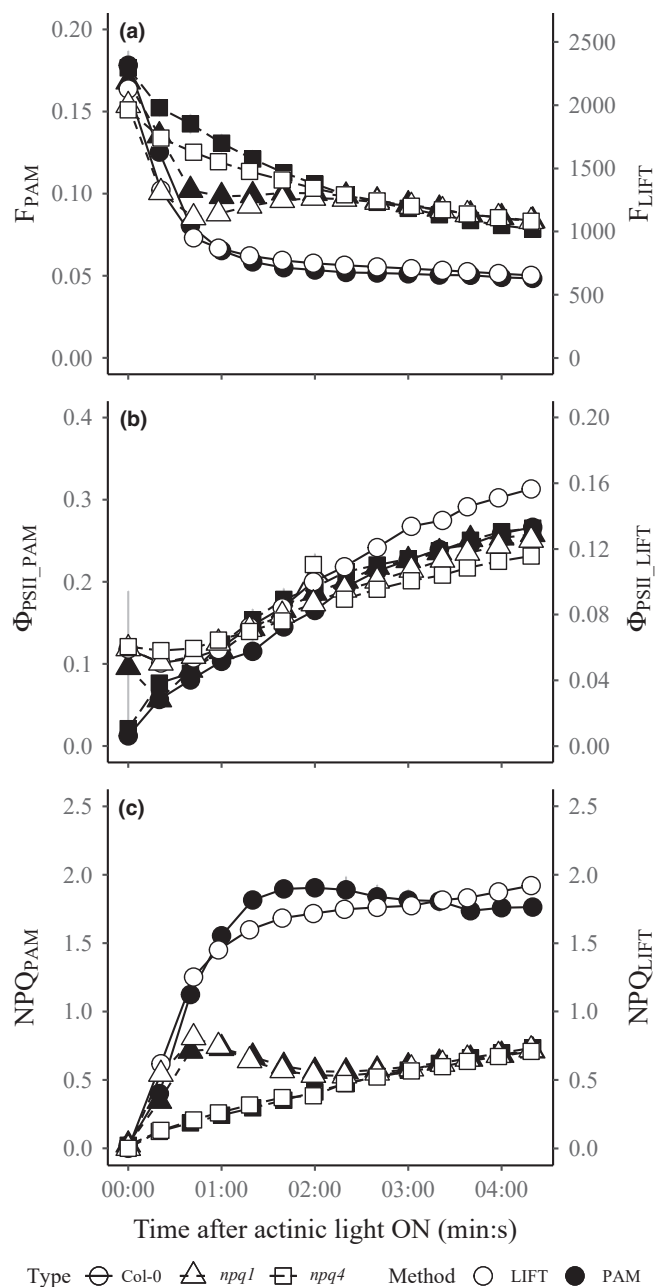


Fig. 1 Fluorescence dynamics after turning on the actinic light ($370 \mu\text{mol m}^{-2} \text{s}^{-1}$), measured in dark-adapted Arabidopsis wild-type (WT) and nonphotochemical quenching (NPQ)-deficient (*npq*) mutants, using active fluorescence measurement techniques. Lines show 4.5-min induction of (a) the fluorescence yield from the pulse-amplitude modulation technique (F_{PAM}) or light-induced fluorescence transients technique (F_{LIFT}), (b) the effective quantum yield of photosystem II (Φ_{PSII}), and (c) nonphotochemical quenching (NPQ) of the Columbia 0 (Col-0) ecotype (circles), and *npq1* (violaxanthin de-epoxidase (VDE)-deficient; triangles) and *npq4* (PsbS-deficient; squares) mutants. Measurements were taken using either pulse-amplitude modulation (PAM, closed symbols) or light-induced fluorescence transients (LIFT, open symbols) techniques. Points indicate the average \pm SE of five plants from each type, measured at room temperature with controlled illumination.

day of cold treatment (Fig. S4e,f). When plants were transferred back to the glasshouse, F_v/F_m slowly increased for all types, suggesting recovery of PSII efficiency (Fig. S5).

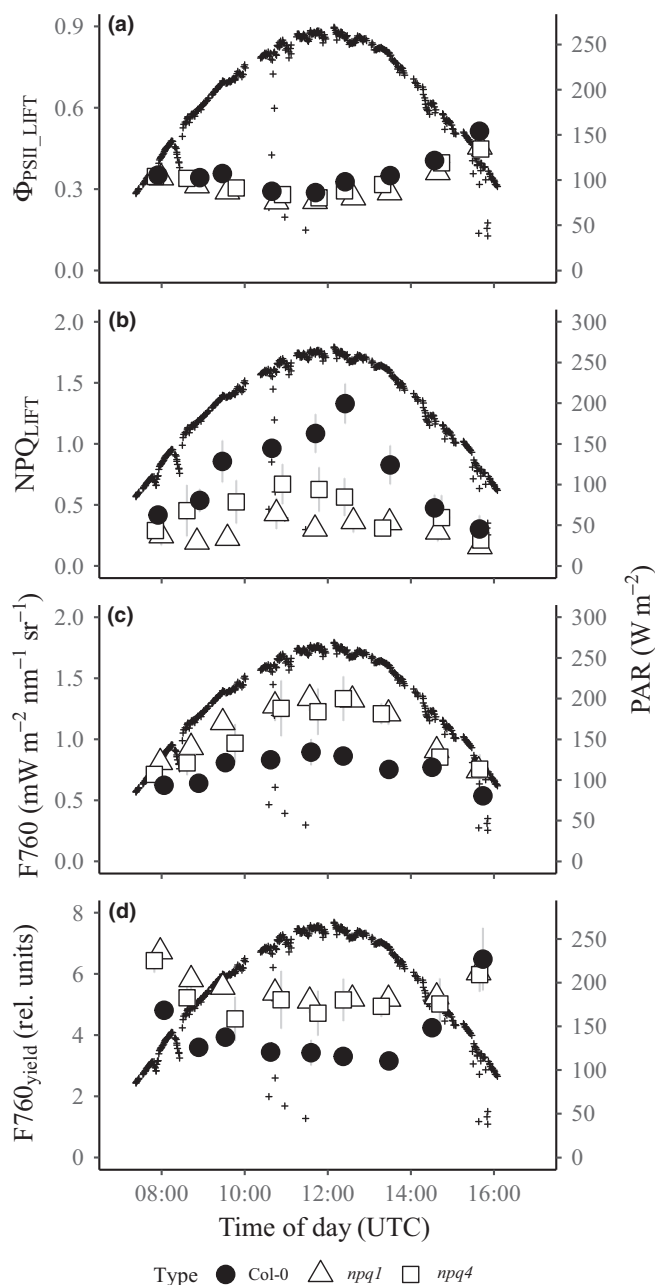


Fig. 2 Diurnal pattern of active and passive fluorescence parameters measured outdoors in the Arabidopsis wild-type (WT) and nonphotochemical quenching (NPQ)-deficient *npq* mutants during the day in summer. Points plotted on the left-hand y-axes are as follows: (a) effective quantum yield of photosystem II from the light-induced fluorescence transients (LIFT) technique (Φ_{PSII_LIFT}), (b) nonphotochemical quenching from the LIFT technique (NPQ_{LIFT}), (c) solar-induced fluorescence emission at 760 nm (F760), and (d) solar-induced fluorescence yield at 760 nm ($F760_{yield}$). Photosynthetically active radiation (PAR) is plotted on the right-hand y-axis. Values are the average \pm SE of four plants from each plant type.

Effect of NPQ mutation in spectrally- and iFLD-resolved SIF

To characterise the effect of PsbS- and Z-deficiency on SIF, spectrally-resolved SIF data for *npq* mutants and WT were compared, and the correlation between iFLD-derived F687 and F760 was

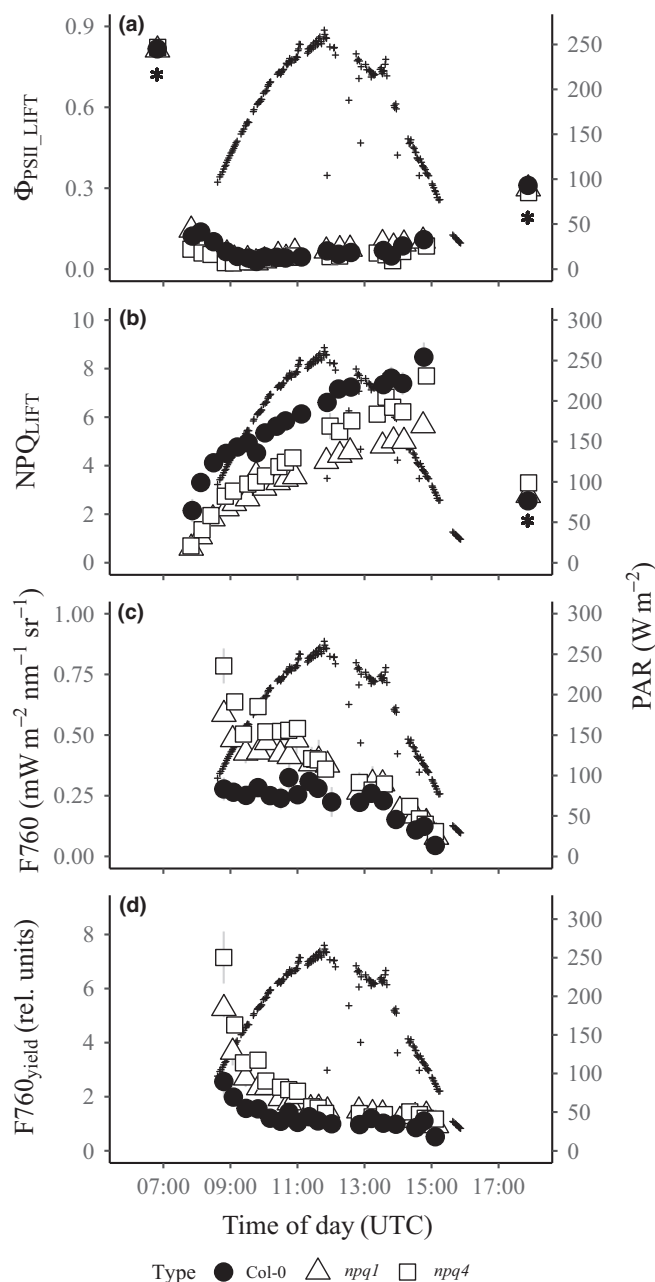


Fig. 3 Diurnal pattern of active and passive fluorescence parameters measured outdoors in the Arabidopsis wild-type (WT) and nonphotochemical quenching (NPQ)-deficient *npq* mutants when exposed to cold day conditions for the first time, mimicking a winter spell effect on plants. Points plotted on the left-hand y-axes are as follows: (a) effective quantum yield of photosystem II from the light-induced fluorescence transients (LIFT) technique (Φ_{PSII_LIFT}), (b) nonphotochemical quenching from the LIFT technique (NPQ_{LIFT}), (c) solar-induced fluorescence emission at 760 nm (F760), and (d) solar-induced fluorescence yield at 760 nm ($F760_{yield}$). Photosynthetically active radiation (PAR) is plotted on the right-hand y-axis. Data points with asterisks are measurements relating to dark-adapted plants in glasshouse conditions. Values are the average \pm SE of three plants from each plant type.

calculated. At leaf level, *npq* mutants showed consistently higher SIF_{yield} at the two fluorescence peaks across the spectrum (Fig. 4a). In outdoor conditions, a strong correlation between F687

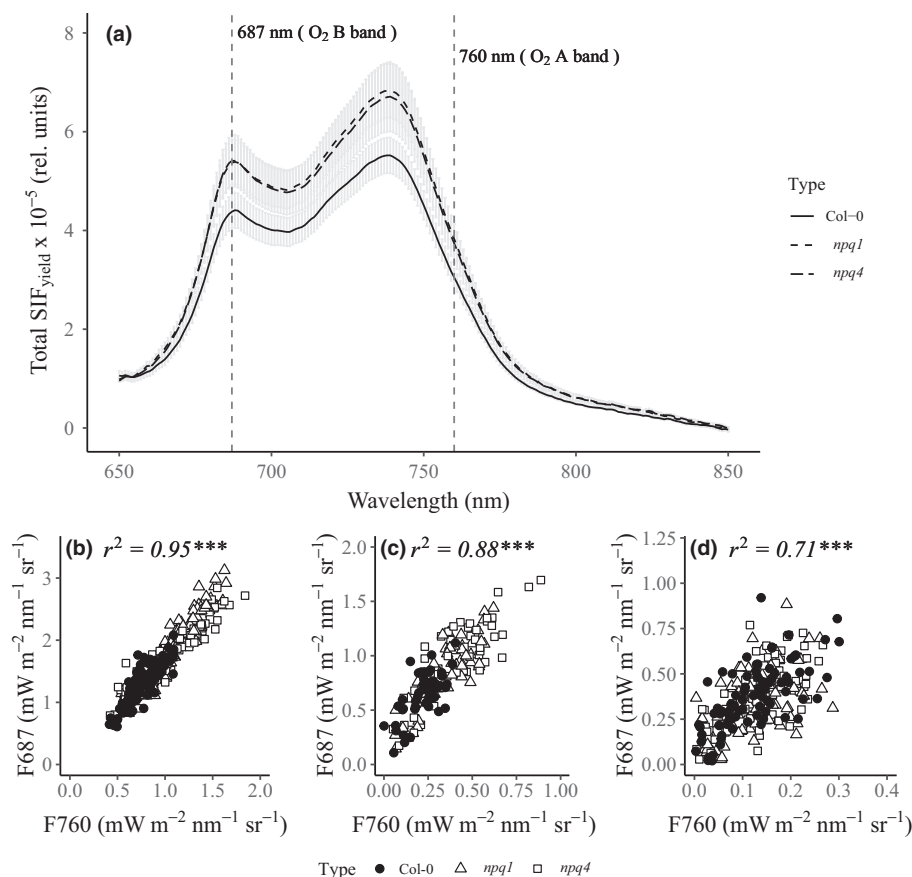


Fig. 4 Relationship between the two fluorescence peaks as affected by the mutation in nonphotochemical quenching (NPQ), presented in full spectra of solar-induced fluorescence yield (SIF_{yield}), as well as solar-induced fluorescence retrieved in O₂A (F760) and O₂B (F687) absorption bands using the improved Fraunhofer Line Depth (iFLD) method. The graphs show the following: (a) total SIF_{yield} spectra, measured in upwelling and downwelling emissions of a single leaf for each plant type; (b) correlation between F687 and F760, measured diurnally during the summer; (c) correlation between F687 and F760, measured diurnally during the cold winter on the first day of exposure; and (d) the second day of exposure. Values are the average \pm SE of four plants from each plant type. Pearson's correlation coefficients (r) are displayed at the top of each graph (*** , $P < 0.001$).

and F760 was observed among all plant types in summer ($r = 0.95$; Fig. 4b). Although we found a similar relationship during the winter spell experiment, more residuals were observed on the first day, with an r of only 0.88 (Fig. 4c), while the correlation was weakest on the second day ($r = 0.71$; Fig. 4d).

Measuring diurnal dynamics of PRI in the WT and *npq* mutants

To determine how PRI is linked to different NPQ components, we calculated PRI from the ρ measurements diurnally resolved in the summer day and winter spell experiments. During the summer, PRI showed a similar diurnal course in WT and *npq4* plants, while the PRI of *npq1* was more or less constant throughout the day (Fig. 5a). In the winter spell, the cold-naïve WT plants had a more stable PRI in the morning, which then decreased in the late afternoon (Fig. 5b). Photochemical reflectance index was higher in *npq1* than in the WT in the morning, then gradually decreased in the afternoon, while *npq4* had an intermediate value between that of the WT and *npq1*. On the second day, all plants showed an identical PRI trend, which followed the diurnal course of PAR (Fig. 5c).

Diurnal measurement of PRI and NPQ in summer showed a clear negative relationship in both the WT and *npq* mutants, although the WT plants reached higher NPQ levels than the mutants (Fig. 6a). By contrast, the negative PRI–NPQ relationship became less distinct in measurements from the winter spell. While the WT had higher NPQ and a lower PRI, the mutants had lower NPQ and a higher PRI (Fig. 6b).

Analysis of spectral reflectance across the visible spectral window

To further investigate the NPQ mechanisms that can be related to changes in ρ signal, a comparison of ρ in WT and *npq* mutants was made, and cluster analysis of diurnal ρ in summer was conducted. There was a clear difference in ρ between the WT and *npq1*, characterized by two distinct peaks – one broadband signal peaking at 520 nm and a narrow range peaking at 700 nm (Fig. 7g). By contrast, there was almost no difference in ρ between the WT and *npq4* plants (Fig. 7h). After cluster analysis, ρ in the WT and *npq4* was almost inseparable, while most *npq1* mutants were clustered together (Fig. 8). The major clustering found was from the WT and *npq4* mutants measured from c. 10:30 h

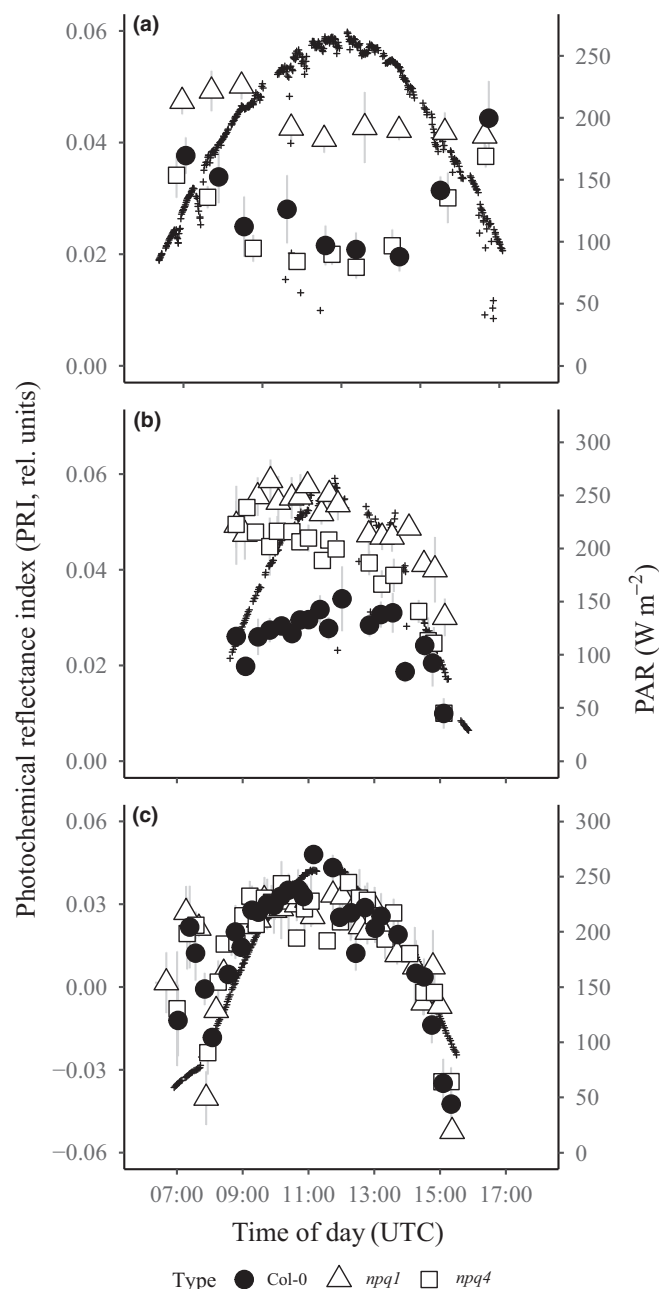


Fig. 5 Diurnal pattern of the photochemical reflectance index (PRI), measured in Arabidopsis wild-type (WT), and violaxanthin de-epoxidase (VDE)-deficient (*npq1*) and PsbS-deficient (*npq4*) mutants during one summer day and two winter days. The graphs show data points collected as follows: (a) during the day in summer, (b) on the first day of exposure to cold conditions and (c) on the second day of exposure to cold conditions. Values are the average \pm SE of three to four plants per genotype.

onwards (branch A, Fig. 8). Interestingly, the clustering also resolved ρ collected at different times of the day. In particular, there was a clear separation of ρ data measured during the morning, at midday and in the late afternoon in branch D (*npq1* cluster) as well as in branch E (Col-0/*npq4* cluster).

Notably, the difference in ρ between branches A and C (Fig. 8) was identical to the pattern of change in ρ ($\Delta\rho$), resolved as

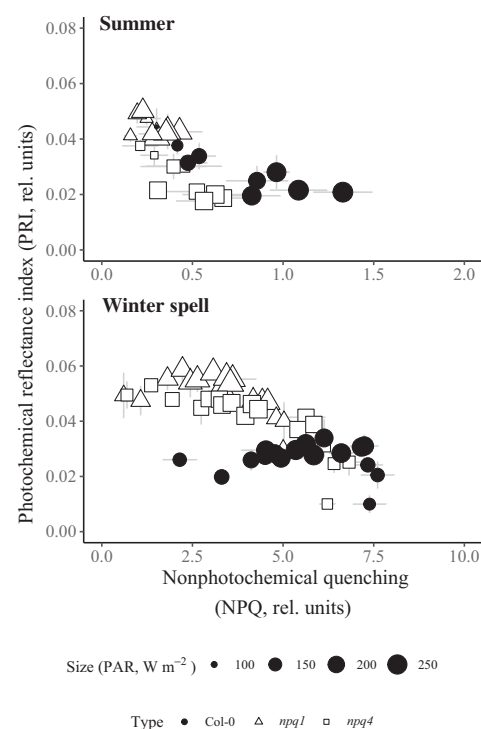


Fig. 6 Relationships between nonphotochemical quenching (NPQ) and photochemical reflectance index (PRI), measured in Arabidopsis wild-type (WT), violaxanthin de-epoxidase (VDE)-deficient (*npq1*) mutant and PsbS-deficient (*npq4*) mutant plants diurnally in summer and during a winter spell. Points are the average \pm SE of three to four plants from each type, repeatedly measured throughout the day. The size of the points is relative to the amount of incoming photosynthetically active radiation (PAR).

the difference between the WT and *npq1* (Fig. 7g). The spectra depicted in Fig. 7(d,f) compare the diurnal changes of ρ from midday to late afternoon; both curves show a broad peak centralized at 560 nm and a narrow peak at 700 nm. Furthermore, the 700 nm peak observed was consistent, yet the magnitude was variable. By contrast, this peak was not observed in the difference between the WT and *npq4* (Fig. 7h). The $\Delta\rho$ at different times of the day, relative to the first measurement in the morning, peaked at 520 nm and 700 nm, while the region from 520 to 650 nm was variable (Fig. S6). It is also worth noting that the 700-nm peak consistently increased between the morning and the afternoon for all plant types.

Relationship of $F760_{\text{yield}}$ to Φ_{PSII} , NPQ and PRI

To quantify the changes in remote-sensing signals that can be related to photochemical and NPQ events, correlations among SIF, PRI, Φ_{PSII} , and NPQ were computed. For the WT plants, $F760_{\text{yield}}$ was found to be positively correlated to Φ_{PSII} but negatively correlated to NPQ during the summer (Figs. 9a, c). The correlation between $F760_{\text{yield}}$ and Φ_{PSII} was slightly stronger than that between $F760_{\text{yield}}$ and NPQ (Table 1). In mutants, $F760_{\text{yield}}$ was directly correlated to Φ_{PSII} and negatively correlated to NPQ, but with lower r than in the WT, with a p -value < 0.05 . By contrast, during sudden cold treatment $F760_{\text{yield}}$ in

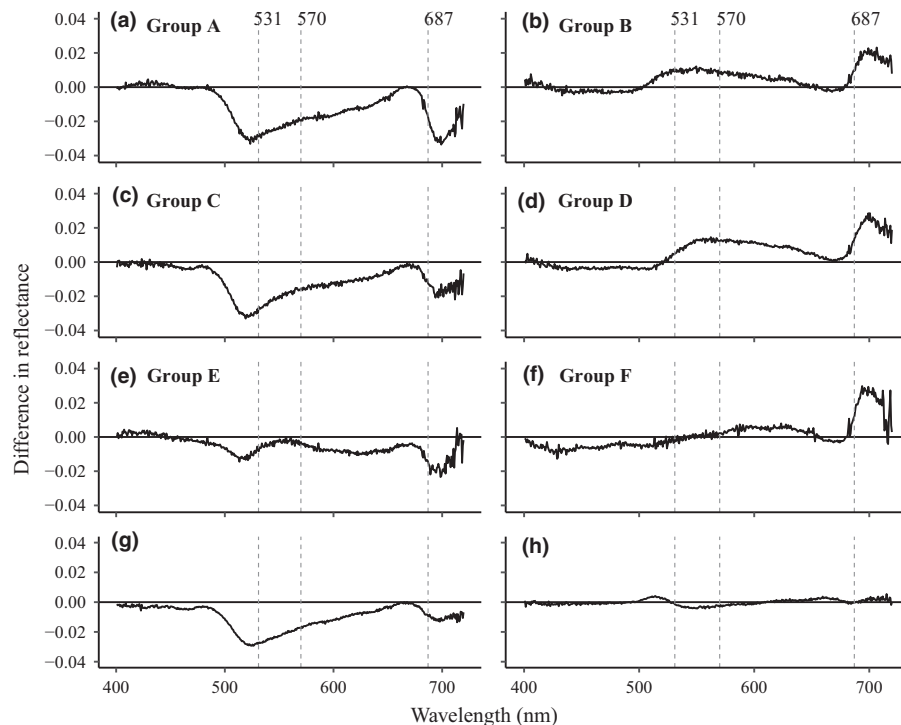


Fig. 7 Spectral characteristics of the difference in spectral reflectance (ρ) between two distinct sub-groupings resolved in the cluster analysis of summer data, as well as the ρ difference between the Arabidopsis wild-type (WT) and nonphotochemical quenching (NPQ)-deficient *npq* mutants. The data show two distinct peaks at ~ 520 nm and 700 nm, and are presented as follows: (a) measurement points associated with strong-minus-weak violaxanthin-antheraxanthin-zeaxanthin cycle (VAZ-cycle) activity; (b) midday minus late afternoon measurement within the violaxanthin de-epoxidase deficient *npq1* mutant cluster; (c) combined Columbia 0 (Col-0, WT) and PsbS-deficient *npq4* mutant minus *npq1* measurements, within the morning cluster; (d) measurements for midday minus late afternoon within the strong VAZ activity cluster; (e) second to third measurements minus the first measurement within the morning cluster from both Col-0 and *npq4*; (f) morning cluster minus *npq1* cluster within the weak VAZ activity cluster; (g) all measurements in summer, during the day, for the WT minus mutant *npq1*; (h) all measurements in summer, during the day, for the WT minus mutant *npq4*. Horizontal dashes indicate reflectance used to calculate photochemical reflectance index (PRI) and solar-induced fluorescence (SIF) retrieval in the O_2B absorption band.

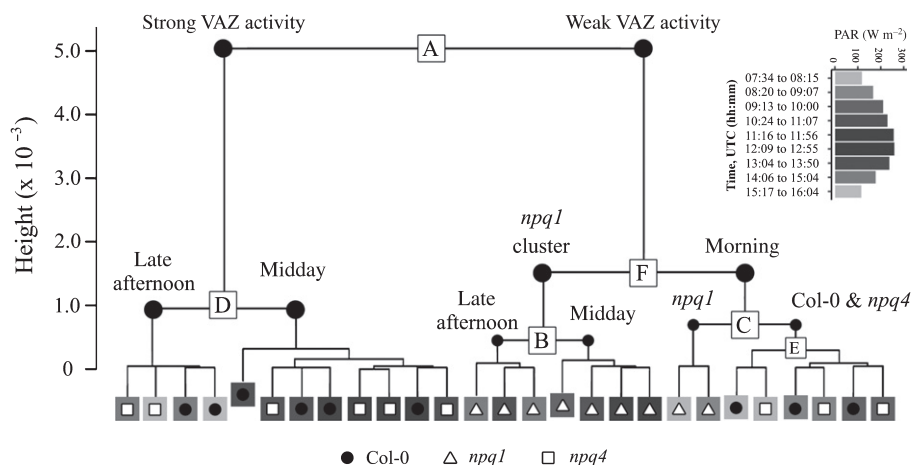


Fig. 8 Cluster analysis of spectral reflectance from 400 nm to 700 nm diurnally, measured during the day in summer, differentiating the Arabidopsis violaxanthin de-epoxidase (VDE)-deficient *npq1* mutant from the wild-type (WT) but not the PsbS-deficient *npq4* mutant. Temporal groupings within plant types were also resolved from morning, mid-day and afternoon measurements. The time range of each measurement window and average light intensity are shown on the upper right-hand side of the figure. Letters indicate the point of separation of spectral reflectance, which was used as the basis for calculating the difference in reflectance previously shown in Fig. 7.

all plant types was positively correlated to Φ_{PSII} only in the morning and then became negatively correlated in the afternoon (Fig. 9b). On the other hand, $F760_{yield}$ was found to have a

strong but nonlinear negative relationship with NPQ ($r = 0.79$) throughout the whole day during the winter spell, for all plant types (Fig. 9d).

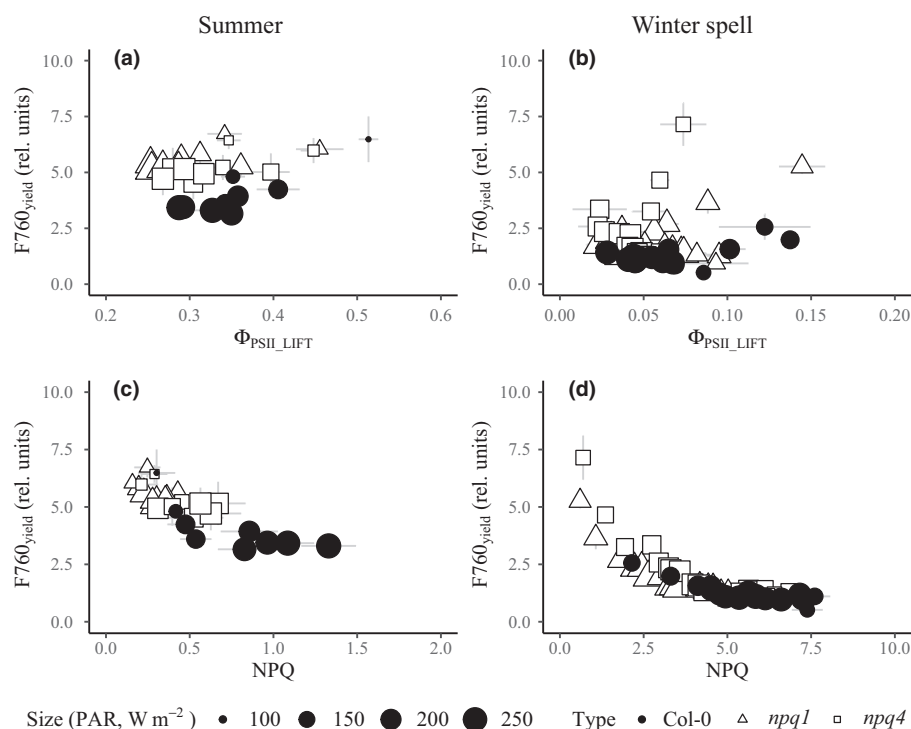


Fig. 9 Relationships between solar-induced fluorescence (SIF) and active fluorescence parameters: solar-induced fluorescence yield at 760 nm ($F760_{\text{yield}}$) vs effective quantum yield of photosystem II from the light-induced fluorescence transients (LIFT) technique ($\Phi_{\text{PSII_LIFT}}$) during (a) summer and (b) a winter spell, as well as $F760_{\text{yield}}$ vs nonphotochemical quenching (NPQ) during (c) summer and (d) a winter spell. Points represent average values \pm SE, measured diurnally in the Arabidopsis wild-type (WT) and *npq* mutants. The size of the points is relative to the amount of incoming photosynthetically active radiation (PAR).

Table 1 Correlation coefficients for solar-induced fluorescence yield at 760 nm ($F760_{\text{yield}}$) and nonphotochemical quenching (NPQ), and effective quantum yield of photosystem II from the light-induced fluorescence transients (LIFT) technique ($\Phi_{\text{PSII_LIFT}}$) and photochemical reflectance index (PRI).

	Summer			Winter spell		
	$F760_{\text{yield}}$ vs NPQ	$F760_{\text{yield}}$ vs Φ_{PSII}	$F760_{\text{yield}}$ vs PRI	$F760_{\text{yield}}$ vs NPQ	$F760_{\text{yield}}$ vs Φ_{PSII}	$F760_{\text{yield}}$ vs PRI
Col-0	−0.74*	0.88**	0.83**	−0.78***	0.05 ^{ns}	0.80***
<i>npq1</i>	−0.58 ^{ns}	0.55 ^{ns}	0.67*	−0.86***	0.11 ^{ns}	0.72***
<i>npq4</i>	−0.64 ^{ns}	0.55 ^{ns}	0.65 ^{ns}	−0.87***	0.13 ^{ns}	0.75***
All points	−0.83***	0.29 ^{ns}	0.67***	−0.79***	−0.05 ^{ns}	0.72***

Test of significance: ^{ns}, not significant ($P > 0.05$); *, $P < 0.05$; **, $P < 0.01$; ***, $P < 0.001$.

The correlation between $F760_{\text{yield}}$ and PRI was stronger during the day in summer than during the winter spell (Table 1). $F760_{\text{yield}}$ was found to be positively related to PRI in WT plants but less distinct in both mutants during summer (Fig. 10a). During sudden cold treatment, $F760_{\text{yield}}$ and PRI had a direct but nonlinear relationship, and the degree of saturation differed across plant types (Fig. 10b). For correlation coefficients, see Table 1.

Discussion

To understand the link between NPQ, photosynthesis and SIF under field conditions, we combined active and passive fluorescence techniques along with changes in ρ . We used Arabidopsis due to its simple canopy structure and mutants with well-defined

NPQ alterations. Firstly, we showed that *npq1* and *npq4* mutants exhibit a similar increase in SIF, indicating that a lack of either PsbS or Z has a similar effect on SIF_{yield} at leaf level (Figs 2c,d, 4a). Secondly, we demonstrated the gradual quenching of SIF during the onset of qI in a winter spell, masking the consequence of NPQ deficiency (Figs 3c,d). Here, we defined sustained NPQ as qI, marked by reduced F_v/F_m as well as a slow recovery. Furthermore, the correlation displayed a better fit between SIF and Φ_{PSII} in summer but a closer relationship between SIF and NPQ during the winter spell (Table 1; Fig. 9). Thirdly, cluster analysis of ρ differentiated *npq1* but not *npq4* from the WT (Fig. 8). We therefore conclude that changes in diurnal ρ are modulated only by the VAZ cycle, eliminating the effect of PsbS-mediated conformational changes of the LHCII to ρ in an outdoor setup. These results are vital for discovering the strengths and

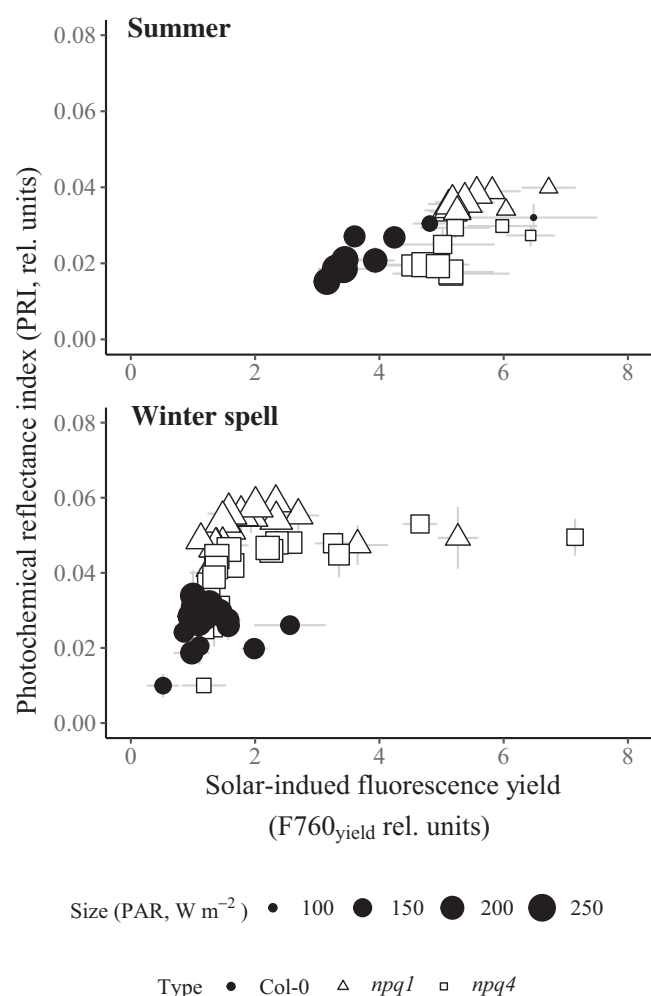


Fig. 10 Relationships between solar-induced fluorescence (SIF) and photochemical reflectance index (PRI), diurnally measured during the day in summer and a winter spell, in the *Arabidopsis* wild-type (WT) and *npq* mutants. Points represent average values \pm SE of three to four plants. The size of the points is relative to the amount of incoming photosynthetically active radiation (PAR).

limitations of SIF and ρ in terms of the remote sensing of NPQ and photosynthesis. Furthermore, they aid our understanding of how to use PRI to estimate the contribution of NPQ to the SIF signal, and how to combine ρ and SIF measurements to understand dynamic photosynthesis under field conditions.

Influence of NPQ deficiency on active and passive fluorescence signals

We showed the consequences of PsbS- and Z-deficiency for active and passive fluorescence signals at leaf level in both a controlled indoor setup and diurnal field conditions in the summer and during a winter spell. PsbS and Z play key roles in the onset of rapidly inducible and reversible qE, and in sustained NPQ in winter (Verhoeven, 2014). We characterized the kinetics of NPQ induction in low light. Absence of Z in the *npq1* mutant reduced the extent of NPQ, but quick induction of NPQ upon

illumination was observed as a result of functional PsbS protein (Fig. 1c). Conversely, the *npq4* mutant showed a slower increase in NPQ which was the effect of VAZ interconversion in the absence of PsbS protein. Our results consistently showed a similar increase in F_{yield} for both *npq* mutants measured in indoor and outdoor conditions (Figs 1a, 2c, 3c), indicating that the extent of NPQ (but not the kinetics) affected diurnal SIF emission. This increase was also consistently visible at the two fluorescence peaks, suggesting that the F687 : F760 ratio is unaffected by changes in NPQ (Fig. 4). Although state transitions may affect this ratio, this was not included in our study as it only occurs under low light levels, and this dynamic is considered less relevant in a remote-sensing context (sensu Porcar-Castell *et al.*, 2014). Nevertheless, in winter, the strength of the correlation between the two fluorescence peaks decreased, which was probably due to a smaller signal-to-noise ratio when SIF was fully quenched (Fig. 4c).

The diurnal observations in summer revealed a dynamic relationship between NPQ, Φ_{PSII} and SIF_{yield} which is consistent with controlled measurements made in a laboratory setting. This coherence also supports the concept that changes in diurnal SIF (in this setup and possibly at larger scales) are not affected by other cellular or leaf level events (e.g. we consider the effect of chloroplast movement on ρ to be negligible on the canopy scale). Fig. 2(d) shows that aside from an absolute increase in SIF_{yield} values in both mutants in the morning, SIF_{yield} was found to be relatively lower in the mutants at the end of the day, and this finding was also coupled with lower Φ_{PSII} (Table S2). This confirms that *npq* mutants with reduced photoprotection are more susceptible to high light stress (Havaux & Niyogi, 1999; Külheim *et al.*, 2002; Li *et al.*, 2002). Thus, SIF_{yield} for the WT was found to recover, while the mutants had a reduced SIF_{yield} when compared to the initial value in the morning (Table S2). We postulate that the qI exhibited by the mutants resulted in a decrease in SIF_{yield}. To test this hypothesis, we controlled the development of qI by exposing the plants to high light and a cold spell during winter. In doing so, SIF quenched equally for all plant types, indicating the onset of qI (Fig. 3), which continued on the second day (Fig. S7). The reduced F_v/F_m and its slow recovery in the glasshouse (Fig. S5) strongly suggest that PSII sustained damage during the winter spell, as well as its corresponding repair.

We have also shown in our setup that a decrease in SIF is always related to an increase in NPQ but is also associated with a decrease in Φ_{PSII} ; however, the coupling of the three processes is not straightforward. We thus developed a conceptual model taking all our measurements into account (Fig. 11, and see Notes S1 and Table S3 on how we translated the measurements into the conceptual model). It is noteworthy that the contribution of basal nonradiative decay is not depicted in the model. The relationship between the three pathways mostly depends on the prevailing environmental conditions. In the WT, SIF was found to be slightly more strongly correlated with Φ_{PSII} than NPQ during the diurnal measurement in the summer condition (Table 1). Conversely, SIF was found to be more strongly correlated with NPQ than Φ_{PSII} during the winter spell, which is predominantly

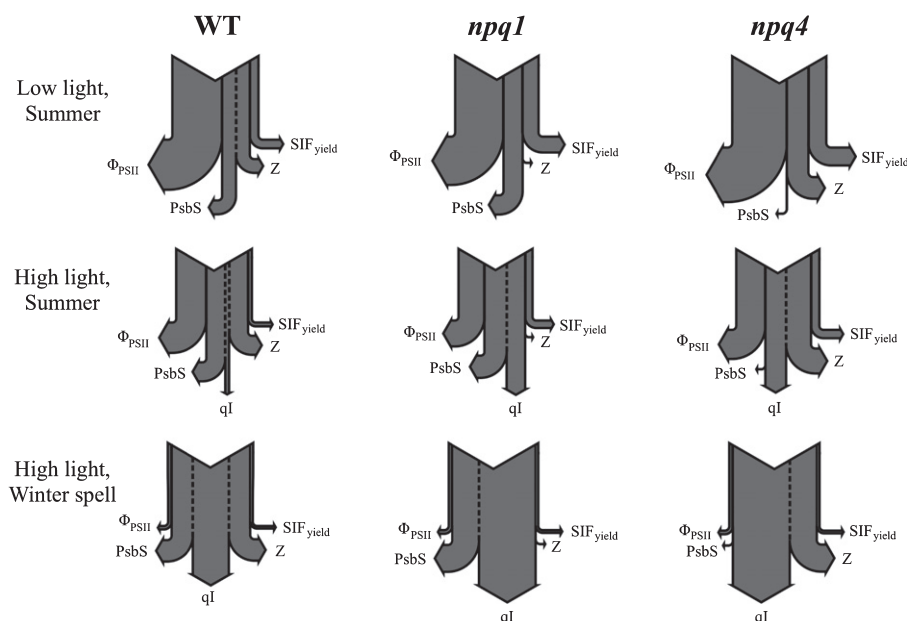


Fig. 11 Schematic representation illustrating the major quenching pathways of absorbed light energy in Arabidopsis wild-type (WT) plants and in the violaxanthin de-epoxidase (VDE)-deficient *npq1* and PsbS-deficient *npq4* mutants under low and high light in summer or during a cold spell. The relative size of each pathway is either based on the observations during the diurnal field experiment (for SIF_{yield} – solar-induced fluorescence yield, and Φ_{PSII} – effective quantum yield of PSII) or estimated by comparison between WT and the mutants (for PsbS, PsbS-dependent quenching; qI , photoinhibitory quenching; Z , zeaxanthin-dependent quenching). Since the quantum yield is not known for the nonphotochemical quenching (NPQ)-related pathways, the width of the pathways does not correspond to their relative contributions. For simplicity, nonregulated energy dissipation is assumed to be similar in the three genotypes under all conditions, and thus is not depicted in this summary.

qI (Fig. 9d). This is different when fluorescence quenching is observed in a dark-adapted leaf, wherein quenching is explained by the Kautsky effect, characterized by an increase in both NPQ and PSII efficiency (Fig. 1b,d). Using the SCOPE model, van der Tol *et al.* (2014) demonstrated that the relative light saturation of PSII affects the relationship between fluorescence and photosynthesis. We hypothesize that this response is due to high light conditions, when Z tends to accumulate. Although the authors showed a strong link between light saturation and rate constant for NPQ, this relationship was purely empirical and did not mechanistically establish the effect of each NPQ component. Our methods have filled this gap using *npq* mutants and have experimentally shown that the lack of either PsbS or Z similarly increases SIF_{yield} in low or high light conditions. Since Z also plays a role in qE , and a lack of PsbS and Z have a similar effect on SIF_{yield} , tracking Z can potentially provide a measure of the relative roles of qE and qZ in SIF quenching.

How can PRI be used as a tool to remotely quantify NPQ contributions to the SIF–photosynthesis relationship?

Photochemical reflectance index is related to NPQ at leaf level (Peñuelas *et al.*, 1995; Gamon *et al.*, 1997; Evain *et al.*, 2004). In remote sensing, changes in ρ can indicate changes in Z accumulation, which is an important component in evaluating de-epoxidation state in the VAZ cycle. We showed that SIF is linearly related to PRI in summer (more importantly in the case of WT plants which naturally exist in the field) (Fig. 10). A weak and nonlinear correlation between SIF and PRI was only found

during the cold spell, when qI , accompanied by changes in other leaf pigments, is suspected to influence the diurnal trend. An overall, albeit uneven, decline in PRI was observed during the cold spell, which is likely due to pigment breakdown (Fig. 5b). It has been shown that seasonal changes in PRI are sensitive to both short and long-term changes in pigment composition (Gamon & Berry, 2012; Wong & Gamon, 2014). Thus, the use of PRI during winter conditions still needs further investigation in order to link with sustained NPQ when Z accumulation is compounded by changes in other pigments in overwintering species (Busch *et al.*, 2009). Kohzuma & Hikosaka (2018) previously showed that PRI in leaf discs changes upon infusion with a pH-controlled buffer. It seems worth exploring how to better retrieve the pH-dependent signal from the ρ measurements, taking into account the pigment and structural changes in canopies. Wong & Gamon (2014) showed that in seasonal observations PRI is strongly related to carotenoid : Chl pigment ratios and minimally attributed to the xanthophyll cycle. In Fig. 5a, the slight decline in PRI observed in the *npq1* mutants was probably due to a build-up of luminal pH as PAR increases. Despite the fact that low luminal pH and PsbS trigger NPQ, we have shown (by tracking in outdoor conditions) a strong correlation between PRI and NPQ (Fig. 6), while SIF and NPQ were found to have a negative relationship (Fig. 9c,d). Since our study was limited to the VAZ cycle, studying the effect of the lutein cycle on SIF and ρ will give a more holistic understanding of the relative $\Delta\rho$ that can be attributed to the NPQ of SIF. Although there are various NPQ mechanisms, the VAZ cycle still plays a major role in regulating the extent of NPQ (Jahns & Holzwarth, 2012).

Clustering clearly separated *npq1* from both WT and *npq4* mutants, which strongly suggests that plant ρ is only sensitive to VAZ activity and not to PsbS-mediated heat dissipation (Fig. 8). While this observation may seem to contradict the report of van Wittenberghe *et al.* (2019), this discrepancy might be due to differences in how $\Delta\rho$ was traced. In particular, they traced $\Delta\rho$ for a maximum of 10 min after actinic illumination, while we monitored $\Delta\rho$ throughout the entire day at *c.* 45 min intervals. Furthermore, diurnal $\Delta\rho$ that is independent of VAZ activity was also resolved in clustering (Fig. 8, branches B and D) which appears to be due to changes at 700 nm, probably resulting from Chl breakdown (Fig. S6). We acknowledge that the lack of pigment data in our study limits further interpretation of this result. Here, we have shown that reflectance at 531 nm is sensitive to changes occurring during the VAZ interconversion (Fig. 7a). By comparing PRI calculated in other spectral regions (Fig. S8), 570 nm showed itself to be a fairly reliable reference band for PRI (first shown by Gamon *et al.*, 1990). PRI on the second day in winter followed light intensity, which was probably a consequence of the changing angle of the sun (Fig. 5c). This suggests that some consideration needs to be given to the effect of leaf albedo and pigment pools when scaling up PRI both temporally and spatially (Wong & Gamon, 2014). Changes in PRI associated with dark conditions or low levels of light would facilitate quantification of pigment changes in a fixed space for remote-sensing applications.

Towards remote sensing of photosynthesis

Changes in SIF due to a dynamic environment are linked to both physical and biological events. Fig. 2(c) shows that SIF is strongly dependent on light intensity. To accurately separate function-related traits from light dependency, emission should be normalized to the fraction of aPAR (fAPAR). Although we only calculated SIF_{yield} by the incoming PAR, it accords with PAM and FluoWat due to the close measurement distance and simple canopy of our target. In remote sensing, SIF_{yield} is compounded by structural effects as well as factors that can influence the ρ -based estimates for light absorption. Future research should, therefore, focus on improving fAPAR estimation from leaf to canopy level, including the escape probability of fluorescence (Zeng *et al.*, 2019).

At canopy level, fAPAR is driven by the complexity of the leaf-area index, leaf angle, leaf clumping, and the pigment composition of the single leaves, which all effect canopy ρ . We have previously shown $\Delta\rho$ at leaf level to be influenced by pigment regulation and that such changes are short-term (diurnal) and long-term (seasonal) responses. This, however, does not directly equate to canopy level as structural effects may have a bigger influence on PRI than physiological dynamics (Gamon *et al.*, 1992; Gitelson *et al.*, 2017). We suggest that changes in PRI can be quantified by removing the canopy effect, as proposed by Hilker *et al.* (2008) and Wu *et al.* (2015). PRI can then be combined with SIF and fAPAR within a spatial domain, and the leaf signal can be scaled-up to the total canopy signal. Pinto *et al.* (2016) was first to report a proof of

concept that high-resolution imaging spectrometers can provide the spatial pattern of SIF in order to quantify photosynthetic functions at canopy level. More recently, Pinto *et al.* (2020) have provided more convincing evidence at a larger spatial scale that the dynamics in PRI and SIF can potentially be linked to photochemical and nonphotochemical events in plants during stress-induced scenarios. The maturity of SIF and ρ measurements at higher spatial and temporal resolutions will enable the scientific community to generate a vast amount of data in order to provide more dynamic empirical correlations between the light-dependent signals and biological events. Our study provides evidence that improves our fundamental understanding of NPQ mechanisms and their contributions, at leaf level, to regulating SIF and PRI during diurnal changes in photosynthesis. Investigation of the influence of Z on PSII efficiency and its consequences for SIF emission is a promising direction for future research, and will create new opportunities to test hypotheses related to the functional role of NPQ in canopy photosynthesis and productivity.

It is well established that SIF can improve estimates of photosynthetic carbon uptake rates and GPP (Guanter *et al.*, 2014; Gu *et al.*, 2019). With the assumption that a homogeneous canopy is a single big leaf, modelling photosynthesis using SIF would require understanding how NPQ is linked to this relationship. While the focus of this paper was to relate SIF to the yield of PSII photochemistry, it is equally important to understand the feedback effect of the Calvin cycle on the rate of electron transport, PSII yield and thus F_{yield} (e.g. stomatal response, carboxylation efficiency, photorespiration, substrate regeneration, etc.). Although ρ reflects only partial NPQ, a parallel survey of light and temperature can be added to numerical simulations to ascertain both the component and mechanism of NPQ involved. We therefore propose that the conceptual model summarized in Fig. 11 should be tested at canopy level and on different species, employing various NPQ strategies.

Acknowledgements



Part of this work was performed within the German-Plant-Phenotyping Network, which is funded by the German Federal Ministry of Education and Research (project identification no. 031A053). Additional support was provided by the SFB/TR 32 D2 subproject, 'Patterns in Soil-Vegetation-Atmosphere Systems: Monitoring, Modelling, and Data Assimilation' (www.tr32.de), funded by the Deutsche Forschungsgemeinschaft (DFG). Data analysis was partly financed by the European Space Agency (ESA) in the frame of the FLEXsense campaign (ESA Contract No. ESA RFP/3-15477/18/NL/NA).


Thanks to Vikas Pingle and Simon Bennertz for helping with data collection, to Beat Keller, MaPi Cendrero-Mateo, Tommaso Julitta and Andreas Burkhart for technical advice on the equipment, and Ladislav Nedbal, Nicolas Zendonadi, Anh Ban, and Maria Paola Puggioni for insightful discussions. The authors declare that they have no conflict of interest. Open access funding enabled and organized by Projekt DEAL.


Author contributions


KA, SM, CJ, OM and UR conceptualized the experiments. KA performed the experiments and analysed the data. DE performed the cluster analysis. KA, SM, OM and UR interpreted the results. KA, UR and SM structured the manuscript and wrote with contributions from OM, DE and CJ.

ORCID

Kelvin Acebron  <https://orcid.org/0000-0002-8523-0256>
Christoph Jedmowski  <https://orcid.org/0000-0003-4647-4896>

Shizue Matsubara  <https://orcid.org/0000-0002-1440-6496>

Onno Muller  <https://orcid.org/0000-0002-0473-5632>

Uwe Rascher  <https://orcid.org/0000-0002-9993-4588>

References

- Ač A, Malenovský Z, Olejníčková J, Gallé A, Rascher U, Mohammed G. 2015. Meta-analysis assessing potential of steady-state chlorophyll fluorescence for remote sensing detection of plant water, temperature and nitrogen stress. *Remote Sensing of Environment* 168: 420–436.
- Alonso L, Gomez-Chova L, Vila-Frances J, Amorós-López J, Guanter L, Calpe J, Moreno J. 2008. Improved Fraunhofer line discrimination method for vegetation fluorescence quantification. *IEEE Geoscience and Remote Sensing Letters* 5: 620–624.
- Alonso L, van Wittenberghe S, Amorós-López J, Vila-Francés J, Gómez-Chova L, Moreno J. 2017. Diurnal cycle relationships between passive fluorescence, PRI and NPQ of vegetation in a controlled stress experiment. *Remote Sensing* 9: 770.
- Atherton J, Nicol CJ, Porcar-Castell A. 2016. Using spectral chlorophyll fluorescence and the photochemical reflectance index to predict physiological dynamics. *Remote Sensing of Environment* 176: 17–30.
- Barton CVM, North PRJ. 2001. Remote sensing of canopy light-use efficiency using the photochemical reflectance index: model and sensitivity analysis. *Remote Sensing of Environment* 78: 264–273.
- Bilger W, Björkman O. 1990. Role of the xanthophyll cycle in photoprotection elucidated by measurements of light-induced absorbance changes, fluorescence and photosynthesis in leaves of *Hedera canariensis*. *Photosynthesis Research* 25: 173–185.
- Bilger W, Björkman O. 1994. Relationships among violaxanthin deepoxidation, thylakoid membrane conformation, and non-photochemical chlorophyll fluorescence quenching in leaves of cotton (*Gossypium hirsutum* L.). *Planta* 193: 238–246.
- Busch F, Hüner NP, Ensminger I. 2009. Biochemical constraints limit the potential of the photochemical reflectance index as a predictor of effective quantum efficiency of photosynthesis during the winter-spring transition in Jack pine seedlings. *Functional Plant Biology* 36: 1016–1026.
- Demmig-Adams B. 1990. Carotenoids and photoprotection in plants: a role for the xanthophyll zeaxanthin. *Biochimica et Biophysica Acta (BBA) – Bioenergetics* 1020: 1–24.
- Demmig-Adams B, Adams WW III. 2006. Photoprotection in an ecological context: the remarkable complexity of thermal energy dissipation. *New Phytologist* 172: 11–21.
- Demmig-Adams B, Adams WI, Logan BA, Verhoeven AS. 1995. Xanthophyll cycle-dependent energy dissipation and flexible photosystem II efficiency in plants acclimated to light stress. *Functional Plant Biology* 22: 249–260.
- Drusch D, Moreno J, Bello UD, Franco R, Goulas Y, Huth A, Middleton EM, Mohammed G, Nedbal L, Rascher U *et al.* 2016. The Fluorescence Explorer mission concept – ESA's Earth Explorer 8. *IEEE Transactions on Geoscience and Remote Sensing* 55: 1273–1284.
- Du S, Liu L, Liu X, Zhang X, Zhang X, Bi Y, Zhang L. 2018. Retrieval of global terrestrial solar-induced chlorophyll fluorescence from TanSat satellite. *Science Bulletin* 63: 1502–1512.
- Evain S, Flexas J, Moya I. 2004. A new instrument for passive remote sensing: 2. Measurement of leaf and canopy reflectance changes at 531 nm and their relationship with photosynthesis and chlorophyll fluorescence. *Remote Sensing of Environment* 91: 175–185.
- Frankenberg C, Fisher JB, Worden J, Badgley G, Saatchi SS, Lee JE, Toon GC, Butz A, Jung M, Kuze A *et al.* 2011. New global observations of the terrestrial carbon cycle from GOSAT: Patterns of plant fluorescence with gross primary productivity. *Geophysical Research Letters* 38: L17706.
- Gamon JA, Berry JA. 2012. Facultative and constitutive pigment effects on the photochemical reflectance index (PRI) in sun and shade conifer needles. *Israel Journal of Plant Sciences* 60: 85–95.
- Gamon JA, Field CB, Bilger W, Björkman O, Fredeen A, Peñuelas J. 1990. Remote sensing of the xanthophyll cycle and chlorophyll fluorescence in sunflower leaves and canopies. *Oecologia* 85: 1–7.
- Gamon JA, Penuelas J, Field CB. 1992. A narrow-waveband spectral index that tracks diurnal changes in photosynthetic efficiency. *Remote Sensing of Environment* 41: 35–44.
- Gamon J, Serrano L, Surfus JS. 1997. The photochemical reflectance index: an optical indicator of photosynthetic radiation-use efficiency across species, functional types, and nutrient levels. *Oecologia* 112: 492–501.
- Gamon JA, Surfus JS. 1999. Assessing leaf pigment content and activity with a reflectometer. *New Phytologist* 143: 105–117.
- Garbulsky MF, Peñuelas J, Gamon J, Inoue Y, Filella I. 2011. The photochemical reflectance index (PRI) and the remote sensing of leaf, canopy and ecosystem radiation-use efficiencies: A review and meta-analysis. *Remote Sensing of Environment* 115: 281–297.
- García-Plazaola JL, Matsubara S, Osmond CB. 2007. The lutein epoxide cycle in higher plants: its relationships to other xanthophyll cycles and possible functions. *Functional Plant Biology* 34: 759–773.
- Gitelson AA, Gamon JA, Solovchenko A. 2017. Multiple drivers of seasonal change in PRI: implications for photosynthesis 2. Stand level. *Remote Sensing of Environment* 190: 198–206.
- Goss R, Lepetit B. 2015. Biodiversity of NPQ. *Journal of Plant Physiology* 172: 13–32.
- Greer DH, Ottander C, Öquist G. 1991. Photoinhibition and recovery of photosynthesis in intact barley leaves at 5 and 20°C. *Physiologia Plantarum* 81: 203–210.
- Gu L, Han J, Wood JD., Chang C Y-Y., Sun Y. 2019. Sun-induced Chl fluorescence and its importance for biophysical modeling of photosynthesis based on light reactions. *New Phytologist* 223: 1179–1191.
- Guanter L, Zhang Y, Jung M, Joiner J, Voigt M, Berry JA, Frankenberg C, Huete AR, Zarco-Tejada P, Lee J-E. 2014. Global and time-resolved monitoring of crop photosynthesis with chlorophyll fluorescence. *Proceedings of the National Academy of Sciences, USA* 111: E1327–E1333.
- Havaux M, Niyogi KK. 1999. The violaxanthin cycle protects plants from photo-oxidative damage by more than one mechanism. *Proceedings of the National Academy of Sciences, USA* 96: 8762–8767.
- Hikosaka K, Noda HM. 2018. Modelling leaf CO₂ assimilation and photosystem II photochemistry from chlorophyll fluorescence and the photochemical reflectance index. *Plant, Cell & Environment* 42: 730–739.
- Hilker T, Coops NC, Hall FG, Black TA, Wulder MA, Nesic Z, Krishnan P. 2008. Separating physiologically and directionally induced changes in PRI using BRDF models. *Remote Sensing of Environment* 112: 2777–2788.
- Horton P, Ruban AV, Rees D, Pascal AA, Noctor G, Young AJ. 1991. Control of the light-harvesting function of chloroplast membranes by aggregation of the LHClI chlorophyll-protein complex. *FEBS Letters* 292: 1–4.
- Jahns P, Holzwarth AR. 2012. The role of the xanthophyll cycle and of lutein in photoprotection of photosystem II. *Biochimica et Biophysica Acta (BBA) – Bioenergetics* 1817: 182–193.
- Joiner J, Yoshida Y, Vasilkov AP, Middleton EM. 2011. First observations of global and seasonal terrestrial chlorophyll fluorescence from space. *Biogeosciences* 8: 637–651.

- Keller B, Vass I, Matsubara S, Paul K, Jedmowski C, Pieruschka R, Nedbal L, Rascher U, Muller O. 2019. Maximum fluorescence and electron transport kinetics determined by light-induced fluorescence transients (LIFT) for photosynthesis phenotyping. *Photosynthesis Research* 140: 221–233.
- Köhler P, Frankenberg C, Magney TS, Guanter L, Joiner J, Landgraf J. 2018. Global retrievals of solar-induced chlorophyll fluorescence with TROPOMI: first results and intersensor comparison to OCO-2. *Geophysical Research Letters* 45: 10456–10463.
- Kohzuma K, Hikosaka K. 2018. Physiological validation of photochemical reflectance index (PRI) as a photosynthetic parameter using *Arabidopsis thaliana* mutants. *Biochemical and Biophysical Research Communications* 498: 52–57.
- Kolber ZS, Prasil O, Falkowski PG. 1998. Measurements of variable fluorescence using FRR technique: Defining methodology and experimental protocols. *Biochimica et Biophysica Acta (BBA) – Bioenergetics* 1367: 88–106.
- Krause GH. 1973. The high-energy state of the thylakoid system as indicated by chlorophyll fluorescence and chloroplast shrinkage. *Biochimica et Biophysica Acta (BBA) – Bioenergetics* 292: 715–728.
- Krause GH. 1988. Photoinhibition of photosynthesis. An evaluation of damaging and protective mechanisms. *Physiologia Plantarum* 74: 566–574.
- Krause GH, Weis E. 1991. Chlorophyll fluorescence and photosynthesis: the basics. *Annual Review of Plant Biology* 42: 313–349.
- Külheim C, Ågren J, Jansson S. 2002. Rapid regulation of light harvesting and plant fitness in the field. *Science* 297: 91–93.
- Li XP, Björkman O, Shih C, Grossman AR, Rosenquist M, Jansson S, Niyogi KK. 2000. A pigment-binding protein essential for regulation of photosynthetic light harvesting. *Nature* 403: 391–395.
- Li XP, Müller-Moulé P, Gilmore AM, Niyogi KK. 2002. PsbS-dependent enhancement of feedback de-excitation protects photosystem II from photoinhibition. *Proceedings of the National Academy of Sciences, USA* 99: 15222–15227.
- Magney TS, Frankenberg C, Fisher JB, Sun Y, North GB, Davis TS, Kornfeld A, Siebke K. 2017. Connecting active to passive fluorescence with photosynthesis: a method for evaluating remote sensing measurements of Chl fluorescence. *New Phytologist* 215: 1594–1608.
- Magney TS, Frankenberg C, Köhler P, North G, Davis TS, Dold C, Dutta D, Fisher JB, Grossmann K, Harrington A *et al.* 2019. Disentangling changes in the spectral shape of chlorophyll fluorescence: Implications for remote sensing of photosynthesis. *Journal of Geophysical Research: Biogeosciences* 124: 1491–1507.
- Maguire AJ, Eitel JU, Griffin KL, Magney TS, Long RA, Vierling LA, Schmiege SC, Jennewein JS, Weygint WA, Boelman NT *et al.* 2020. On the functional relationship between fluorescence and photochemical yields in complex evergreen needleleaf canopies. *Geophysical Research Letters* 47: 1–9.
- Maxwell K, Johnson GN. 2000. Chlorophyll fluorescence – a practical guide. *Journal of Experimental Botany* 51: 659–668.
- Müller P, Li XP, Niyogi KK. 2001. Non-photochemical quenching. A response to excess light energy. *Plant Physiology* 125: 1558–1566.
- Nichol CJ, Rascher U, Matsubara S, Osmond B. 2006. Assessing photosynthetic efficiency in an experimental mangrove canopy using remote sensing and chlorophyll fluorescence. *Trees* 20: 9–15.
- Niyogi KK, Grossman AR, Björkman O. 1998. *Arabidopsis* mutants define a central role for the xanthophyll cycle in the regulation of photosynthetic energy conversion. *The Plant Cell* 10: 1121–1134.
- Öquist G, Huner NP. 2003. Photosynthesis of overwintering evergreen plants. *Annual Review of Plant Biology* 54: 329–355.
- Osmond B, Chow WS, Wyber R, Zavafer A, Keller B, Pogson BJ, Robinson SA. 2017. Relative functional and optical absorption cross-sections of PSII and other photosynthetic parameters monitored in situ, at a distance with a time resolution of a few seconds, using a prototype light-induced fluorescence transient (LIFT) device. *Functional Plant Biology* 44: 985–1006.
- Owens TG, Shreve AP, Albrecht AC. 1992. Dynamics and mechanism of singlet energy transfer between carotenoids and chlorophylls: light harvesting and non-photochemical fluorescence quenching. In: Murata N, ed. *Research in Photosynthesis*. Dordrecht, The Netherlands: Kluwer Academic, 179–186.
- Peñuelas J, Filella I, Gamon JA. 1995. Assessment of photosynthetic radiation-use efficiency with spectral reflectance. *New Phytologist* 131: 291–296.
- Pieruschka R, Albrecht H, Muller O, Berry JA, Klimov D, Kolber ZS, Malenovsky Z, Rascher U. 2014. Daily and seasonal dynamics of remotely sensed photosynthetic efficiency in tree canopies. *Tree Physiology* 34: 674–685.
- Pinto F, Celesti M, Acebron K, Alberti G, Cogliati S, Colombo R, Radoslaw J, Matsubara S, Miglietta F, Palombo A *et al.* 2020. Dynamics of sun-induced chlorophyll fluorescence and reflectance to detect stress-induced variations in canopy photosynthesis. *Plant, Cell & Environment* 43: 1637–1654.
- Pinto F, Damm A, Schickling A, Panigada C, Cogliati S, Müller-Linow M, Balvora A, Rascher U. 2016. Sun-induced chlorophyll fluorescence from high-resolution imaging spectroscopy data to quantify spatio-temporal patterns of photosynthetic function in crop canopies. *Plant, Cell & Environment* 39: 1500–1512.
- Porcar-Castell A, Tyystjärvi E, Atherton J, van der Tol C, Flexas J, Pfündel EE, Moreno J, Frankenberg C, Berry JA. 2014. Linking chlorophyll and fluorescence to photosynthesis for remote sensing applications: mechanisms and challenges. *Journal of Experimental Botany* 65: 4065–4095.
- R Core Team. 2013. *R: A language and environment for statistical computing*, v.3.5.0. R Foundation for Statistical Computing, Vienna, Austria. [WWW document] URL <http://www.R-project.org/> [accessed 19 May 2017].
- Rascher U, Agati G, Alonso L, Cecchi G, Champagne S, Colombo R, Damm A, Daumard F, de Miguel E, Fernandez G *et al.* 2009. CEFLES2: the remote sensing component to quantify photosynthetic efficiency from the leaf to the region by measuring sun-induced fluorescence in the oxygen absorption bands. *Biogeosciences* 6: 1181–1198.
- Rascher U, Alonso L, Burkart A, Cilia C, Cogliati S, Colombo R, Damm A, Drusch M, Guanter L, Hanus J *et al.* 2015. Sun-induced fluorescence – a new probe of photosynthesis: first maps from the imaging spectrometer HyPlant. *Global Change Biology* 21: 4673–4684.
- Rossini M, Nedbal L, Guanter L, Ač A, Alonso L, Burkart A, Cogliati S, Colombo R, Damm A, Drusch M *et al.* 2015. Red and far-red Sun-induced chlorophyll fluorescence as a measure of plant photosynthesis. *Geophysical Research Letters* 42: 1632–1639.
- Ruban AV. 2016. Non-photochemical chlorophyll fluorescence quenching: mechanism and effectiveness in protecting plants from photodamage. *Plant Physiology* 170: 1903–1916.
- Sun Y, Frankenberg C, Jung M, Joiner J, Guanter L, Köhler P, Magney T. 2018. Overview of solar-induced chlorophyll fluorescence (SIF) from the orbiting carbon observatory-2: retrieval, cross-mission comparison, and global monitoring for GPP. *Remote Sensing of Environment* 209: 808–823.
- van der Tol C, Berry JA, Campbell PKE, Rascher U. 2014. Models of fluorescence and photosynthesis for interpreting measurements of solar-induced chlorophyll fluorescence. *Journal of Geophysical Research: Biogeosciences* 119: 2312–2327.
- van Wittenberghe S, Alonso L, Malenovsky Z, Moreno J. 2019. In vivo photoprotection mechanisms observed from leaf spectral-absorbance changes showing VIS–NIR slow-induced conformational pigment bed changes. *Photosynthesis Research* 142: 283–305.
- van Wittenberghe S, Alonso L, Verrelst J, Hermans I, Delegido J, Veroustraete F, Valcke R, Moreno J, Samson R. 2013. Upward and downward solar-induced chlorophyll fluorescence yield indices of four tree species as indicators of traffic pollution in Valencia. *Environmental Pollution* 173: 29–37.
- Verhoeven A. 2014. Sustained energy dissipation in winter evergreens. *New Phytologist* 201: 57–65.
- Verrelst J, van der Tol C, Magnani F, Sabater N, Rivera JP, Mohammed G, Moreno J. 2016. Evaluating the predictive power of sun-induced chlorophyll fluorescence to estimate net photosynthesis of vegetation canopies: a SCOPE modeling study. *Remote Sensing of Environment* 176: 139–151.
- Vilfan N, van der Tol C, Verhoef W. 2019. Estimating photosynthetic capacity from leaf reflectance and Chl fluorescence by coupling radiative transfer to a model for photosynthesis. *New Phytologist* 223: 487–500.
- Wong CY, Gamon JA. 2014. Three causes of variation in the photochemical reflectance index (PRI) in evergreen conifers. *New Phytologist* 206: 187–195.
- Wu C, Huang W, Yang Q, Xie Q. 2015. Improved estimation of light-use efficiency by removal of canopy structural effect from the photochemical reflectance index (PRI). *Agriculture, Ecosystems & Environment* 199: 333–338.

- Yang X, Tang J, Mustard JF, Lee JE, Rossini M, Joiner J, Munger JW, Kornfeld A, Richardson AD. 2015. Solar-induced chlorophyll fluorescence that correlates with canopy photosynthesis on diurnal and seasonal scales in a temperate deciduous forest. *Geophysical Research Letters* 42: 2977–2987.
- Zarco-Tejada PJ, Miller JR, Mohammed GH, Noland TL, Sampson PH. 2000. Chlorophyll fluorescence effects on vegetation-apparent reflectance: II laboratory and airborne canopy-level measurements with hyperspectral data. *Remote Sensing of Environment* 74: 596–608.
- Zeng Y, Badgley G, Dechant B, Ryu Y, Chen M, Berry JA. 2019. A practical approach for estimating the escape ratio of near-infrared solar-induced chlorophyll fluorescence. *Remote Sensing of Environment* 232: 111209.

Supporting Information

Additional Supporting Information may be found online in the Supporting Information section at the end of the article.

Fig. S1 Growing conditions of the Arabidopsis WT and *npq* mutants before field measurement in summer and winter conditions.

Fig. S2 Illustration of diurnal measurement combining both active and passive fluorescence measurements and spectral reflectance.

Fig. S3 Recorded diurnal light intensity and temperature during field measurement on summer and winter days.

Fig. S4 Diurnal trend of F687 in summer and winter field conditions.

Fig. S5 Recovery of F_v/F_m after exposure to a cold spell for 2 d.

Fig. S6 Diurnal change in spectral reflectance in the WT, *npq1* and *npq4* mutants, relative to the first measurement.

Fig. S7 Diurnal trends for active and passive fluorescence parameters measured during the second day of exposure to outdoor winter conditions.

Fig. S8 Diurnal pattern of two different PRI calculations measured in summer and a simulated cold spell during winter.

Notes S1 Considerations for developing quantitative values for the conceptual model in Fig. 11.

Table S1 List of abbreviations used in this manuscript.

Table S2 SIF_{yield} and Φ_{PSII} during the morning, midday and afternoon, measured for all Arabidopsis plant types.

Table S3 Final input values for the Sankey diagram shown in Fig. 11.

Please note: Wiley Blackwell are not responsible for the content or functionality of any Supporting Information supplied by the authors. Any queries (other than missing material) should be directed to the *New Phytologist* Central Office.